

Additive Manufacturing of Microfluidic Components via Wax Extrusion

Philip Schneider¹, Viktor Sukhotskiy¹, Tyler Siskar², Liam Christie¹, Ioannis Karamelas³,
Edward P. Furlani^{1,4}, Kwang. W. Oh¹

¹Dept. of Electrical Engineering

²Dept. of Physics

³Flow Science Inc., Santa Fe NM

⁴Dept. of Chemical and Biological Engineering

University at Buffalo SUNY, Buffalo NY, email: kwangoh@buffalo.edu

ABSTRACT

This paper presents an innovative application of the fused deposition modeling (FDM) technique in wax printing of microfluidic structures. Preliminary experimental fabrication and characterization of printed wax ridges, as well as thermo-fluidic computational fluid dynamic (CFD)-based modeling of the printing process are presented. The 3D CFD model solves the Navier-Stokes and heat transfer equations for flowing wax and accounts of solidification as the wax cools. The CFD modeling provides fundamental understanding of the printing physics, to enable rational tuning of critical process parameters toward optimization of the ridge printing process. This wax-based printing technique uses a printing style similar to that of the polymer-based FDM 3D printing process wherein a wax extruder tip, filled with molten beeswax is translated across a printing substrate using precise computer-based motion control to create fluidic circuit positive molds at the microscale. The molds can be used to fabricate fluidic circuit components. The wax-based FDM 3D printing technique and the accompanying CFD model provide a rational design testbed for future fabrication of microfluidic components.

Keywords: Wax-Based Microfluidics, Flow modeling

1 INTRODUCTION

There are currently numerous methods for microfluidic device fabrication, the most prevalent using soft lithography [2]. However, this technique often requires expensive equipment, toxic compounds, time consuming fabrication steps and a clean room environment. As such, practitioners continue to investigate alternate methods to overcome the limitations of the current standard in microfluidic device fabrication [3]. One such approach is three-dimensional (3D) printing of microfluidic devices. Fused deposition modelling (FDM) has been extensively applied in the fields of rapid prototyping and 3D printing, but these techniques have mostly been used for the fabrication of low melting point plastics and polymers. In addition, techniques that utilize wax patterning, or wax based microfluidics, have proven to be a potential vehicle to overcome traditional fabrication difficulties. Wax microfluidics generally consists of either constructing a hydrophobic barriers or creating a master mold design using wax [4]. Wax is a desirable medium for microfluidics, due to its low cost,

nontoxic, and dissolvable properties opening up a range of applications from microfluidic mixer [5], valves [6] and 3D models [7].

This paper examines a low cost, rapid prototyping, wax based contact printing microfluidic fabrication system that can lower the cost of microfluidic device fabrication and testing. The system extrudes wax, via a print nozzle, across a substrate surface in a predesigned microfluidic pattern. The wax lines, or ridges, on the glass act as a mold over

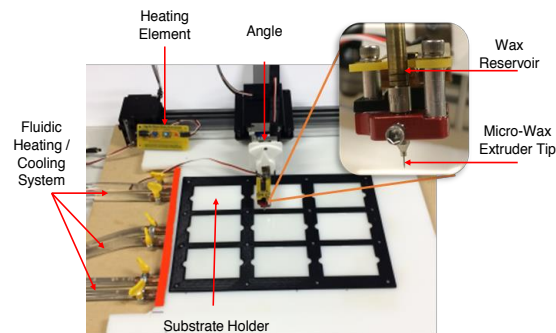


Figure 1. (a) Photograph of the wax printer consisting of X-Y mechanical actuation of a heated aluminum extruder tip (inset). An array of glass slides held by a 3D printed frame was mounted to an acrylic board.

which PDMS is poured as shown in (Fig. 1). When solidified the PDMS is peeled off and the negative imprint is now molded into the PDMS. This can then be used as a microfluidic device, in the same manner as a soft lithographic process. The system's basic operating parameters: printing speed, print substrate material, wax extruder tip angle, wax composition and wax temperature, are critical parameters that have been quantified in terms of their impact on the printing performance. Among numerous performance criteria are the wax ridge shape uniformity, surface roughness, feature size, and cross sectional area. However, there are a number of additional testing criteria that are not practical to quantify using physical experimentation due to time and costs.

To compliment this physical wax printing system, and to aid in the experimentation and prototyping of more unique testing criteria, a 3D thermo-fluidic CFD model was developed. This model enables the user to evaluate a microfluidic wax pattern quickly and inexpensively,



Figure 2. Overview of the extrusion tip and: (a) Photograph of the wax extruder tip printing a straight beeswax ridge on a glass substrate at room temperature. (b) Typical wax cross-sectional profile as measured by a profilometer.

allowing direct observation of physical parameters such as substrate temperature, extruder tip temperature, viscosity of wax, surface finish, solidification dynamics, and their effect on the printed wax ridge. Unique experimental conditions that would be expensive and time consuming to test can be examined at a much faster rate. Microscale fluid flow models have proven valuable in the analysis of current microfluidic systems. There is considerable interest in modeling the relationship between paraffin wax and fluid flow for applications in microfluidics [8]. In this case, the computational model needs to allow for system parameter variation that enables the rational design of the final printed structure. For instance, a change in substrate temperature affects the height of the wax ridge (extreme temperatures beyond current system capabilities). Substrate material (i.e. quartz, gold, platinum, silicon), also affects the shape of the wax ridge. The model should predict the resolution, uniformity, and functionality of the printed system to advance understanding of the underlying physical phenomena that govern the contact-based wax printing process. Ultimately, this model will accelerate the rational design of the system and allow for exploration of additional applications.

2 PHYSICAL SYSTEM OVERVIEW

The wax printing prototype used for experimental testing is built from a modified x-y-z actuation system (AxiDraw, Evil Mad Scientist, Sunnyvale, CA, USA) and allows for real time microfluidic device mold prototyping using a contact based wax printing method. This machine, originally used for calligraphy, was modified by retrofitting a wax extrusion tip and an electronic heating unit to allow for temperature control, and by extension, the viscosity of the wax to be altered as shown in Fig. 2. A unique aspect of this setup is that it allows the extruder tip to be exchanged with tips of various inner diameters (3x Fine (254 μm), Extra fine (457.2 μm), Fine (533.4 μm), Medium (660.6 μm), and Heavy (889 μm)). This enables printing of features with different heights, thickness, and widths. An acrylic base board with a 3D printed glass slide holder held the substrate in place while undergoing printing. A system

overview is shown in Fig. 1. This customizable mechanism allows for wax to be extruded on any surface or material, given that the beeswax can adhere to it. To date, testing has included glass, paper, silver, copper, plastic, wood and aluminum substrates. Underneath the printing base lies a tube piping system through which cold and hot fluid is pumped. Cold fluid acts to prevent wax spreading, thus increasing minimum channel feature size, and hot fluid allows for a re-flow of the wax to remove non-uniformities in the channel cross-sectional profile.

The flexibility of this systems parameter variation goes a step further with the ability to manually adjust the substrate temperature. Temperature control was accomplished by using a portable fluidic heating and cooling unit (ThermaZone Continuous Thermal Therapy, Innovate Medical Equipment, Cleveland, OH, USA). This allowed for temperature control of the print substrate, cooling or heating, utilizing a continuous fluidic flow system. Copper pipes were inserted beneath the base that allowed for hot/cold water to flow through. Through conduction, the base and print substrates were evenly affected by the temperature change of the pipes. The temperature ranges between 2°C to 51.7°C. Variable temperature is important for controlling parameters.

As shown in Eq.1, known as Washburn's equation, there is a direct relationship between wax spreading (i.e. the wax channel width and height) and the printing parameters)

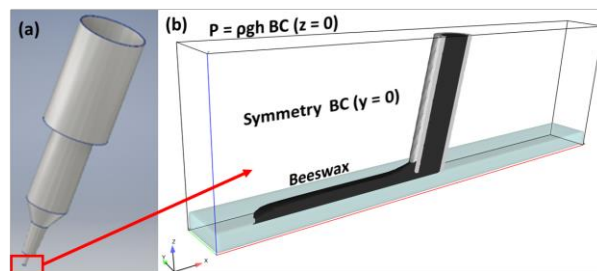


Figure 3. (a) Diagram of an extruder tip used for simulations. (b) Computational domain used for simulating wax extrusion.

$$L^2 = \frac{\gamma D t}{4\eta} \quad (1)$$

Where t is the time for a liquid with a dynamic viscosity η and surface tension γ to penetrate a distance L into the capillary whose pore diameter is D . For instance, adjusting the wax temperature affects the dynamic viscosity, which is related to how far the wax spreads on the substrate. In addition, the temperature of the writing substrate affects the rate at which the wax solidifies. All of these parameters ultimately affect the performance of the

system. **Figure 2** shows the zoomed in image of the wax contact printing method on a glass substrate.

3 COMPUTATIONAL MODEL

A CFD analysis of the wax extrusion process was performed to gain insight into the critical physical phenomena of this approach. The FLOW-3D CFD software package (www.flow3d.com) was used for the analysis. In this model, the Navier-Stokes equations (Eq 2) are solved using the volume of fluid (VOF) method [9] to track the free-surface of the molten wax and additional equations to track solidification of the wax based on porous media drag. The solidification model uses a solid fraction variable to determine the state of solidification point-wise within a fluid. The solid fraction is simply the ratio of the solidified material to the total material in the computational domain. When the solid fraction is below a critical value at a given point, a Darcy type drag force is added to the Navier-Stokes equation,

$$\rho \left(\frac{\partial}{\partial t} + \mathbf{v} \cdot \nabla \right) \mathbf{v} = -\nabla p + \mu \nabla^2 \mathbf{v} \quad (2)$$

Where ρ and μ are the density and viscosity of the liquid wax, and \mathbf{v} and p are the velocity and pressure. At points where the solid fraction is above the critical value, the drag is set to infinity and the liquid behaves as a solid. In order to calculate the solid fraction, the model tracks the temperature of the wax and the relevant temperature fluxes via a thermos-fluidic heat transfer equation,

$$\rho c_p \left(\frac{\partial T}{\partial t} + \mathbf{v} \cdot \nabla T \right) = k \nabla^2 T \quad (3)$$

where, c_p is the specific heat of wax, T is the absolute temperature and k is the thermal conductivity.

The computational domain (CD) for this model is shown in **Fig. 3**. In this model, the lowest part of the extrusion tip is modelled by applying a hydrostatic pressure condition

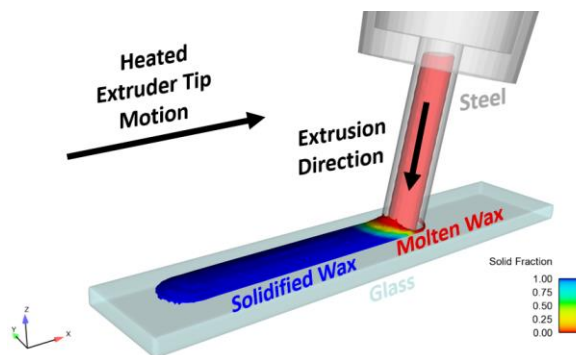


Figure 4. FLOW-3D thermofluidic simulation of the extrusion and solidification of beeswax during tip motion.

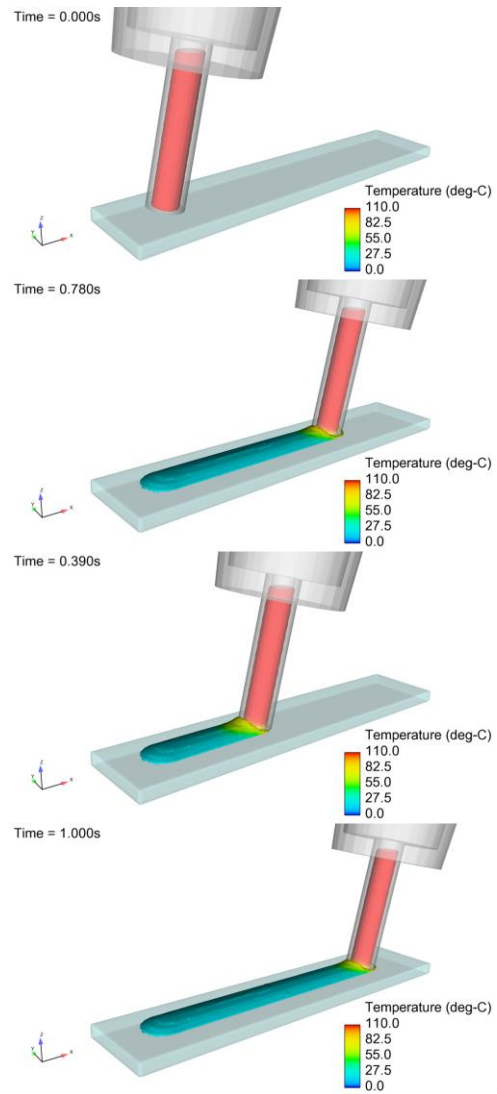


Figure 5. Time snapshots of the simulated temperature distributions of the beeswax ridge during printing.

$\rho g h$ on the top boundary of the CD, which reduces computational expense. Here, g is gravitational acceleration and h is the height of the fluid above the x - y plane of the CD. This pressure, driven by gravity, represents the remainder of the fluid above this small part of the nozzle and acts as the extrusion mechanism for the process. The CD is cut in half along the y - z plane and a symmetry boundary condition is applied to reduce computational expense.

Temperature-dependent fluidic and thermal physical parameters were used for the analysis [10, 11]. The beeswax was deposited directly onto a 20°C glass substrate with a fixed position. The extrusion tip was moved at a constant velocity of 2 mm/s and tipped at an angle of 10 degrees from the normal to the substrate. The total simulation time was 1 second, resulting in a wax ridge 2 mm in length.

4 RESULTS

The profilometer-measured elevations of a several experimentally printed wax ridges were used to validate the model. The operating parameters used in the model were as follows: extruder tip velocity = 2mm/s, a contact angle = 80° (10° from the surface normal), wax temperature = 110°C, and substrate temperature = 20°C. The simulation results are shown in Fig. 5. The predicted cross sectional area of a deposited ridge is compared with measured data in Table I, which shows an error of 10.67%. This error can be attributed to a number of factors ranging from the temperature variation of the substrate as well as the external environmental condition that affect the wax solidification rate such as humidity and room temperatures. Finally, there was a variation between the wax temperatures of the models, and in turn the kinematic viscosity of the wax. The difference between temperatures results in a 3.5 mm²/s change in kinematic viscosity, which in turn affects the solidification rate of the wax.

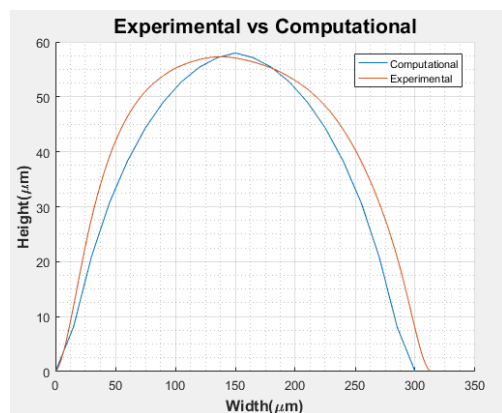


Figure 6. Time snapshots of the simulated temperature distributions of the beeswax ridge during printing.

	Computational	Physical	% Error
Wax Height (μm)	57.982	57.306	1.18%
Cross Sec. Area (μm ²)	11,568	12,951	10.67%

Looking at Washburn's equation the distance the wax expands before solidification is a direct function of the temperature of the wax. This is a high attribution of the error rate in our model which will be corrected in future testing.

5 CONCLUSION

This paper demonstrates the implementation of a rigorous 3D CFD model and its comparison to the real world physical system. The accuracy of this comparison

was 89.33% in terms of cross-sectional area, and 98.82% in terms of wax ridge height. This simulation provided a fundamental understanding of the process and can be used to explore aspects of the system that cannot be easily implemented in a practical setting. This ranges from printing parameters like substrate material (platinum, gold), extreme temperature variations, new part testing prior to fabrication (micro extruder tip), and/or printing material, such as various wax compounds or polymers. Ultimately, this simulation enables proof-of-concept in advanced of fabrication and the rational design, and optimization of new products. Future testing includes simulation optimization, as well as continued experimentation validation of the model.

REFERENCES

- [1] P. Schneider, B.B., D. Koh, A. Wang, A. Trimper, K. Oh, *Low Cost, Rapid Prototyping, Wax Based Microfluidics- Serial Dilution*. NanoTec 2017, 2017.
- [2] Duffy, D.C., et al., *Rapid Prototyping of Microfluidic Systems in Poly(dimethylsiloxane)*. Analytical Chemistry, 1998. **70**(23): p. 4974-4984.
- [3] Bhattacharjee, N., et al., *The upcoming 3D-printing revolution in microfluidics*. Lab on a Chip, 2016. **16**(10): p. 1720-1742.
- [4] He, Y., et al., *Fabrication of paper-based microfluidic analysis devices: a review*. RSC Advances, 2015. **5**(95): p. 78109-78127.
- [5] Li, Z.a., et al., *Fabrication of PDMS microfluidic devices with 3D wax jetting*. RSC Advances, 2017. **7**(6): p. 3313-3320.
- [6] Diaz-Gonzalez, M., C. Fernandez-Sanchez, and A. Baldi, *Multiple actuation microvalves in wax microfluidics*. Lab on a Chip, 2016. **16**(20): p. 3969-3976.
- [7] Wang, W., S. Zhao, and T. Pan, *Lab-on-a-print: from a single polymer film to three-dimensional integrated microfluidics*. Lab on a Chip, 2009. **9**(8): p. 1133-1137.
- [8] Salih, N.M., et al., *Surface Tension Analysis of Cost-Effective Paraffin Wax and Water Flow Simulation for Microfluidic Device*. Advanced Materials Research, 2014. **832**: p. 773-777.
- [9] Hirt, C. W., and B. D. Nichols. 'Volume of Fluid (VOF) Method for the Dynamics of Free Boundaries', J. Comput. Phys, 1981, pp. 201-225.
- [10] Lew, D.D. *Physical Properties of Beeswax and Paraffin*. Global Warming 2018; Available from: <https://www.drdarrinlew.us/global-warming/physical-properties-of-beeswax-and-paraffin-wax.html>
- [11] Ramnanan-Sigh, R., *Formulation & Thermophysical Analysis of a Beeswax Microemulsion & The Experimental Calculation of its Heat Transfer Coefficient*, City College of New York, CUNY, 2012; Available from: https://academicworks.cuny.edu/cc_etds_theses/115/